Journal of Japan Society of Civil Engineers, Ser.
B1 (Hydraulic Engineering), Vol. 70, No. 4, I_19-I_24, 2014.

EXPERIMENTAL AND NUMERICAL STUDY OF FLUSHING CHANNEL FORMATION IN SHALLOW RESERVOIRS

Taymaz ESMAEILI[1], Tetsuya SUMI[2] and Sameh A. KANTOUSH[3]

[1]Member of JSCE, Ph.D. Student, DPRI, Kyoto University (Gokasho, Uji, Kyoto 611-0011, Japan)
[2]Member of JSCE, Professor, DPRI, Kyoto University (Gokasho, Uji, Kyoto 611-0011, Japan)
[3]Associate Professor, Department of Civil Engineering, German University in Cairo (New Cairo City, Cairo, Egypt)

Sediment flushing is one of the proposed methods for preserving the storage capacity of dam reservoirs. In flushing with water level drawdown, the incoming flood erodes a flushing channel in the deposited sediment. Flow pattern as well as flushing channel formation procedure in shallow reservoirs is complex phenomenon due to the dynamic interaction between flow field and bed changes. In the present study, the flow field and flushing channel formation procedure were investigated in various shallow reservoir geometries using physical experiments and numerical simulation. A fully 3D numerical model which applies Finite Volume Method (FVM) was utilized. Reasonable agreement was found between the numerical and experimental outcomes. The results would be useful to understand the influence of geometry on flow pattern and flushing process to conduct more efficient sediment management strategies.

Key Words**:** *Shallow reservoirs, 3D numerical simulation, reservoir sedimentation, sediment flushing.*

1. INTRODUCTION

Sediment deposition is the principal problem affecting the useful life of reservoirs. A decreased storage volume reduces the reservoir function for flood control purpose, electricity production and water supply. This loss of storage volume represents a huge economic loss and the reduction of flood control benefits[1)]. Also, the amount of storage loss varies dramatically from river basin to river basin due to the different forest cover and geological conditions[2)]. The sedimentation problem is serious for small and medium sized reservoirs with high sediment inflow.

In order to control the reservoir sedimentation, different approaches such as bypassing, dredging, flushing, sluicing and upstream sediment trapping have been developed. Among several techniques, the flushing and sluicing plays an important role in the sediment removal and reduction, as they are efficient hydraulic sediment removal technique to restore the reservoir storage capacity[1),3)].The success of flushing depends on the sediment characteristics, the hydraulic and hydrological conditions[1)~3)]. Sediment flushing with drawdown is ongoing at Dashidaira & Unazuki dam reservoirs in the Kurobe River as pioneer cases in Japan.

Sediment flushing in reservoirs involves several complex processes. During the flushing with drawdown, bottom outlets are opened to generate and accelerate unsteady flow towards the outlet. This process will initiate the progressive and retrogressive erosion pattern in tail and delta reaches of the reservoirs respectively[4)]. The mentioned process finally leads to the flushing channel formation and flushing out both fine and coarse sediments through reservoirs. Detailed theoretical explanation of flushing channel formation in reservoir delta is scarce. The characteristic of the flushing channel when the water level is drawndown can be briefly introduced by the location, shape, width, side and longitudinal slope[5)]. For practical purposes, the pre-assessment of the flushing channel development characteristic using a 3D numerical model would be beneficial to optimize the sediment flushing operation as well as the flood risk management in reservoirs.

Application of numerical models enables the reservoir owners to assess the impacts of upcoming

flushing event in the reservoir and implement the appropriate measures aimed to enhance the flushing efficiency. When it is necessary to assess the distribution of shallow parts, deep parts and sandbar areas for reservoir sediment management strategies, numerical models other than one-dimensional one should be used[6]. Many calculation methods based on 2D models have been developed for practical problems in rivers[7]. However, the one and two dimensional models are not able to directly simulate the secondary current influences. Also, quasi-3D models can be categorized whether the shallow water flow assumed or not[8]. Still it is difficult for advanced quasi-3D models to reproduce complex 3D flows[9].

Subsequently, 3D numerical models are necessary to simulate the complex 3D flow pattern and bed variation in rivers and reservoirs. In the present study, a fully 3D numerical model was employed to analyze the surface flow field in a series of rectangular shallow reservoirs and then the flushing channel formation and evolution trend were simulated in the aforementioned reservoirs. The next step would be simulating the sediment flushing process in a real prototype scale to enhance the flushing efficiency by employing various measures.

2. MATERIALS AND METHODS

(1) Experimental setup

The experimental tests were carried out in a rectangular basin with the maximum inner length of 6m and width of 4m. Also, the inlet and outlet rectangular channel width was 0.25m. The different shallow reservoir geometry achieved experimentally by moving the PVC plate walls. A moveable frame with 4m long was mounted on the side walls of reservoir for installing the measurement devices.

Ultrasonic probes were utilized for measuring the water level and Large Scale Particle Image Velocimetry technique (LSPIV) was used for measuring the surface velocity field. Ultra Sonic Velocity Profiler device (UVP) was employed for providing the 3D flow velocity measurements as well. Bed topography was measured by a miniature echo sounder which was mounted on the moveable frame and could scan the whole geometry domain. Moreover, two SOLITAX sc sensors which utilize the ultrasonic approach were installed for measuring the suspended sediment concentration.

(2) Experimental conditions

The non-uniform crushed walnut shells were added to the mixing tank during the test to represent the suspended sediment. The median size of this non-cohesive light-weight and homogenous grain material was 50 μm with σ_g of 2.4 and density of 1500 kg/m³. The Froude number range set to ($0.05 \leq Fr \leq 0.43$) whereas the Reynolds number range was ($14000 \leq Re \leq 28000$) to ensure the subcritical and fully developed turbulent flow. The flow discharge rate (Q), suspended sediment concentration (C) and water depth (h) were constant for all experiments as 0.007m³/s, 3gr/L and 0.2m respectively.

The test procedure had three different stages. In the first stage, the shallow reservoirs was filled with clear water and after reaching to the stable state, in the second phase, the mixture of water-sediment was drained by the gravity into the water-filled reservoir for a total period of 4.5 hours. In the third phase, two types of flushing with and without drawdown were performed. The final bed topography from the second phase was considered as the initial bed for two types of flushing. Afterwards, the clear water inflow introduced into the reservoir to evaluate the surface velocity pattern, flushing channel evolution, channel location as well as the flushing efficiency. As for the flushing without drawdown in run T1, the clear water without sediment was injected into the reservoir with the constant hydraulic condition (Q=0.007m³/s and h=0.2m). The drawdown flushing was conducted by opening the outlet gate and lowering the water level to half of the initial level for runs T8, T11 and T13. Then, pump was turned on by keeping a constant discharge (Q=0.007m³/s and h=0.1m). **Table 1** shows geometrical attributes of various geometries employed in the present study.

It was found that the flushing channel formation is a very rapid procedure that takes less than 3 hours.

(3) Numerical model

A fully 3D numerical model was employed in this study. The numerical model solves the Reynolds-averaged Navier-Stokes equation together with mass and momentum conservation in three dimensions to compute the water motion for turbulent flow as follows.

$$\frac{\partial U_i}{\partial x_i} = 0 \tag{1}$$

$$\frac{\partial U_i}{\partial t} + U_j \frac{\partial U_i}{\partial x_j} = \frac{1}{\rho}\frac{\partial}{\partial x_j}\left(- P\delta_{ij} + \rho \upsilon_T \left(\frac{\partial U_i}{\partial x_j} + \frac{\partial U_j}{\partial x_i}\right)\right) \tag{2}$$

in which i=1, 2, 3 is the representative of three directions; where U_j is the Reynolds-averaged velocity over time t, x is the spatial geometrical scale, ρ is the water density, P is the Reynolds-averaged pressure, δ_{ij} is the Kronecker delta and ν_T is the turbulent eddy-viscosity. For transforming the partial equations into algebraic

Table 1 Experimental configuration. L and B are the length and width, Pr is the wetted perimeter, A is the surface area of the basin, AR equals to (L/B) and SF is the shape factor.

Case	L(m)	B(m)	Pr(m)	A(m²)	AR	SF=(Pr/√A)×AR
T 1	6	4	19.5	24	1.5	5.97
T 8	6	2	15.5	12	3	13.42
T 11	5	4	17.5	20	1.25	4.89
T 13	3	4	13.5	12	0.75	2.92

equations, the finite volume method is applied as discretization method. The change in water-levels was based on calculated pressure field. The pressure was extrapolated to the water surface and the pressure difference between a surface node and the downstream node was used to estimate the water elevation difference [10]. The turbulence is modeled by the standard k-ε model, using the constant empirical values[11]. The unknown pressure field is also calculated employing Semi Implicit Method for Pressure-Linked Equations, (SIMPLE) method[12]. The grid is adaptive and moves with change in the bed and water levels.

The Dirichlet boundary condition for the water inflow (logarithmic velocity distribution) was used while for the water and sediment outflow zero-gradient boundary condition was assumed. As for the boundary condition at the walls, where there is no water flux, the empirical wall laws were used as follows:

$$\frac{U}{u^*} = \frac{1}{\kappa}\ln\left(\frac{30y}{k_s}\right) \tag{3}$$

where the shear velocity is denoted u^*, κ is the Karman constant equal to 0.4, y is the distance to the wall and k_s is the equivalent roughness.

The sediment transport computation for simulating the morphological change is divided into suspended and bed load transport. Suspended load is calculated by solving the transient convection-diffusion equation formula (**Eq. 4**) and bed load is simulated by Van Rijn formula[13] (**Eq. 5**).

$$\frac{\partial c}{\partial t} + U_j\frac{\partial c}{\partial x_j} + w\frac{\partial c}{\partial z} = \frac{\partial}{\partial x_j}(\Gamma_T\frac{\partial c}{\partial x_j}) \tag{4}$$

Where U is the water velocity, w is the fall velocity of sediments, Γ is the turbulent diffusivity and can be expressed by (**Eq. 6**) and c is the sediment concentration over time t within the spatial geometrical scales x and z.

$$\frac{q_{b,i}}{d_i^{1.5}\sqrt{\frac{(\rho_s-\rho_w)g}{\rho_w}}} = 0.053\frac{\left[\frac{\tau-\tau_{c,i}}{\tau_{c,i}}\right]^{1.5}}{d_i^{0.3}\left[\left(\frac{(\rho_s-\rho_w)g}{\rho_w\nu^2}\right)\right]^{0.1}} \tag{5}$$

where $q_{b,i}$ is sediment transportation rate for the ith fraction of bed load per unit width, d_i is the diameter of the ith fraction, τ is the shear stress, $\tau_{c,i}$ is the critical shear stress for d_i which was calculated from the Shield's curve, ρ_s is the density of sediment, ρ_w is the density of the water, g is the gravity acceleration and ν is the kinematic viscosity.

$$\Gamma_T = \frac{\nu_T}{Sc} \tag{6}$$

where Sc is the Schmidt number representing the ratio of eddy viscosity coefficient ν_T to diffusion coefficient and set to 1.0 as default.

In order to compute the suspended sediment concentration in the cells close to the bed, a specified concentration was used as boundary condition[14].

3. RESULTS AND DISCUSSIONS

(1) Flow pattern simulation

The complexity of velocity measurement with high spatial resolution in different shallow reservoir geometries pronounces the necessity to conduct the numerical modeling along with physical experiments. As for the real cases, modeling the flow field will provide us useful information about the areas with the potential erosion and deposition during the anticipated floods. This information would be useful for flood risk assessment in reservoirs near the urban areas.

The mesh cell size for case T1, T8, T11 and T13 in X and Y direction was 5cm×2.5cm, 5cm×1.5cm, 5cm×2cm and 2.5cm×1cm respectively. Considering the 11 cells for vertical grid distribution, the total number of cells were 218240, 174460, 220000 and 528000 respectively. For model validation, the simulated surface flow velocity field was compared to that of measured experimentally.

The final bed morphology, which was obtained after the sediment flushing, was introduced to the model as the boundary condition and then three-dimensional flow field was calculated. Time step was calibrated as 2 seconds for run T1 and T8 whereas it was 1 second for T11 and T13. Bed roughness was fixed as 0.00015m which equals to 3 times of median sediment size. **Fig. 1** illustrates the transversal flow velocity (Uy) contours over the depth along with the secondary flow velocity vectors for case T8 and T13. **Fig**. **2** shows the simulated and measured surface velocity magnitudes (V) in m/s and distribution pattern with uniform scaled vectors.

Fig. 3 illustrates the simulated streamwise and transversal surface velocity distribution versus

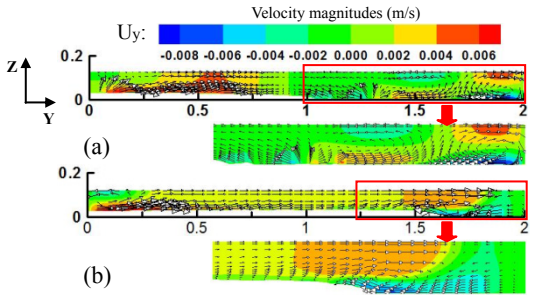

Fig. 1 Transversal velocity distribution over the depth at the middle cross section of (a) T8 and (b) T13.

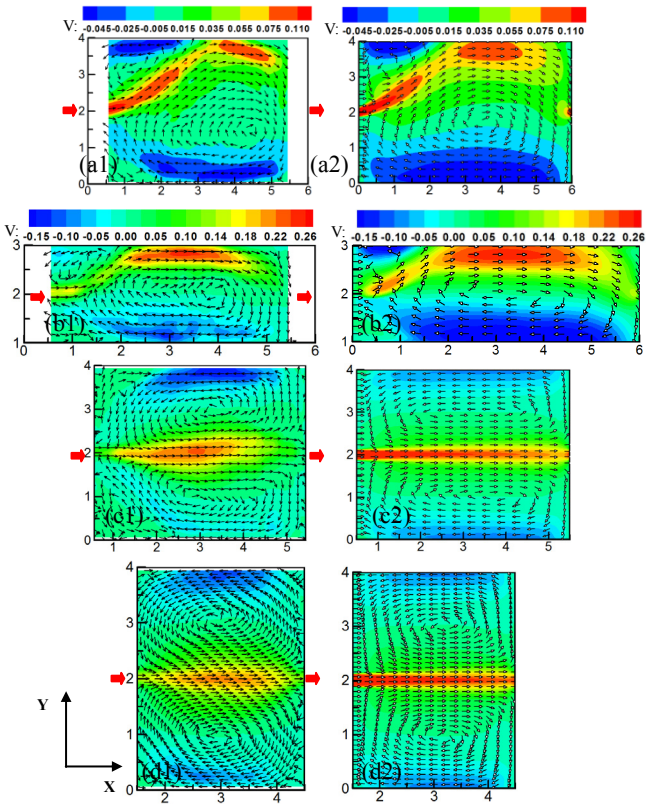

Fig. 2 Left: The measured surface velocity magnitudes (V) and velocity vectors for runs (a1) T1, (b1) T8, (c1) T11 and (d1) T13 respectively and right: corresponding simulated velocity magnitudes and velocity vectors.

measured one in the middle part of the channel length. As can be clearly observed form the **Fig**. **2** and **Fig**. **3**, the model could simulate the surface flow velocity pattern almost similar to the measured one by reproducing the dominant aspects such as the main flow jet trajectory and location of the reverse flow as well as the main vortices and corner gyres. However, simulation results show the higher flow velocity magnitudes than observations over the main jet trajectory for all cases and over reverse flow in case of T1 and T8. Also, the size of the upstream corner gyres in case T11 is smaller than the measured one because of the straighter simulated surface velocity pattern than hydraulic model test.

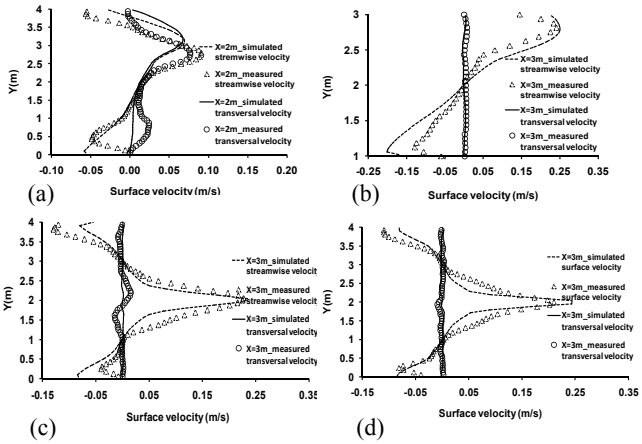

Fig. 3 The measured streamwise and transversal surface velocity at the middle area of the channel versus simulated surface velocity for (a) T1, (b) T8, (c) T11 and (d) T13.

(2) Simulation of flushing with drawdown

Numerical outcomes as well as the observations in experimental runs revealed that if the water level is drawndown significantly, the flow starts to erode the bed progressively propagating to the downstream and retrogressively from the outlet towards upstream. The progressive trend was faster than retrogressive one. In the meantime, the initial flushing channel deepened and widened rapidly due to the strong jet flow and subsequent erosion. Then, after formation of initial flushing channel along the reservoir length, the rate of channel widening reduced noticeably until reaching a dynamic stable condition over the whole channel length. The mentioned process is very quick up to the slow widening stage so that the measurement of the bed evolution was difficult. Subsequently, numerical model outcomes along with the final measured results in the equilibrium stage utilized to further description of the process. **Fig. 4** demonstrates the

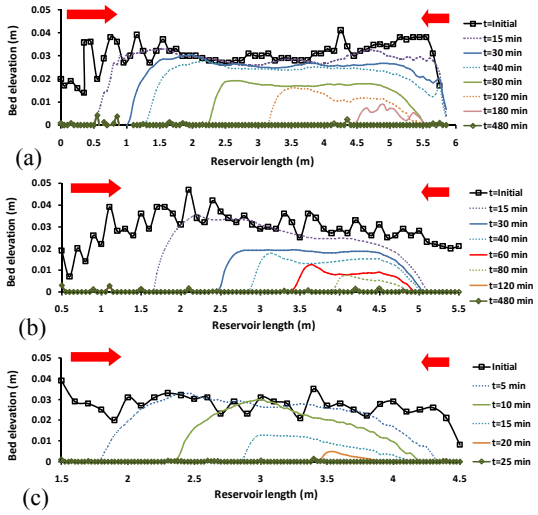

Fig. 4 Longitudinal development of flushing channel along the centerline for (a) T8, (b) T11 and (c) T13 provided by numerical model.

longitudinal progressive and retrogressive pattern, reproduced numerically, along the centerline of T8, T11 and T13 reservoirs. Numerical computation was performed until starting the slow channel widening stage. Thus, as soon as cumulative sediment pass variation within 30 minutes interval became smaller than 1%, simulations were stopped.

Described flushing channel formation process was consistent with the real observations during the drawdown flushing in Dashidaira and Unazuki dam reservoirs. The side bank erosion and lateral development of flushing channel in the middle length of the reservoirs has been shown in **Fig. 5**.

Fig. 6 illustrates the plan view of final measured bed level contours (Z) after 48 hours and simulated one after initiating the slow channel widening stage.The size, shape, location and evolution pattern of the flushing channel was simulated up to the early stage of slow widening phase. It takes long time to simulate whole 48 hours by 3D numerical model. The characteristics of flushing channel components, more or less, have been reproduced by the numerical model except for run T8 in which the location of the channel was different than measured one. Although the geometry was symmetric, the channel did not develop along the shortest path from inlet to outlet during the experiment. The reason can be attributed to the accidental small disturbance in the inflow discharge distribution along the inlet channel width. In such a condition, location of the flushing channel is very likely to change from the centerline of the reservoir. As the numerical model assumes the uniform inflow discharge distribution and symmetric initial condition, the flow direction would be straight and subsequently model is not able to break the symmetry of input data.

As to the run T11 and T13, both experimental measurements and numerical outputs show that the channel width increased in the downstream direction similar to a T shape head (**Fig. 6(b2) & (c2)**. The longer simulation period, the similar channel width as well as T head shape will be reproduced close to the outlet.

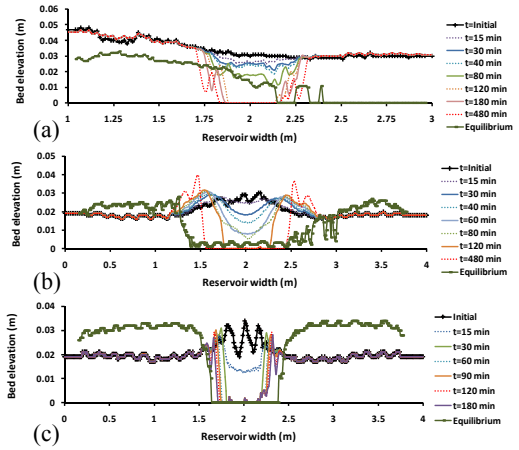

Fig. 5 Bank erosion and lateral development of flushing channel for (a) T8, (b) T11 and (c) T13.

(3) Flushing efficiency

In this study the Flushing Efficiency (FE) was defined as the volume ratio of flushed out sediment to cumulative deposited sediment after the deposition (second) phase. **Fig. 7** illustrates the temporal sediment discharge change in milliliter per second and cumulative sediment pass through the outlet for run T8, T11 and T13. The erosion rate is very high at early stage owing to the rapid deepening and widening of flushing channel. Then, the sediment discharge rate decreases remarkably as the initial flushing channel was formed along the whole length of the reservoir. Afterwards, during the

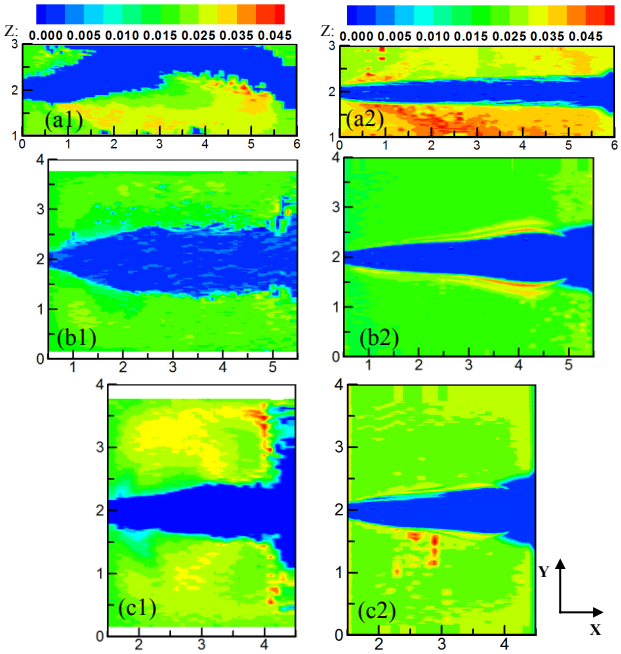

Fig. 6 Left: The measured flushing channel shape and location for (a1) T8, (b1) T11 and (c1) T13 respectively and right: the corresponding simulated results.

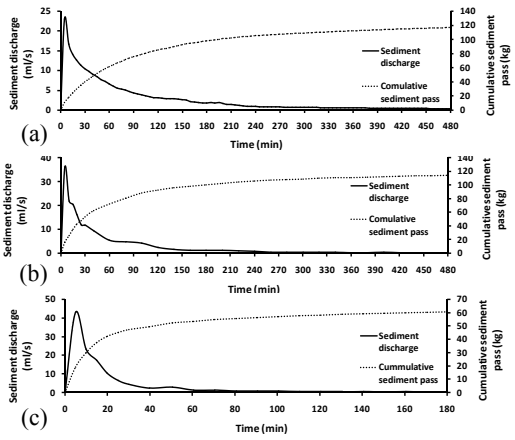

Fig. 7 Calculated flushed out sediment for the run (a) T8, (b) T11 and (c) T13.

slow channel widening stage, the sediment discharge rate remains almost stable. The measured and calculated FE has been plotted versus reservoir shape factor in **Fig. 8**.

In case of drawdown flushing, FE increases significantly with the higher reservoir shape factor in experimental runs. In other word, the flushing efficiency with drawdown will be high for narrow reservoir geometries. On the contrary, the FE in flushing without drawdown is low because of very local erosion pattern in the inflow and outflow area.Right illustration in **Fig.8** clearly shows local erosion during the flushing without drawdown.

The numerical model outputs showed slightly lower FE rate than measured ones in Case T11 and T13. The main reason is due to the computation stop as soon as slow widening stage starts. Nevertheless, in case of T8, measured and numerically modeled FE has great discrepancy. This is because of the wide meandering flushing channel formation in the experiments whereas the width and length of the simulated straight flushing channel is smaller than that of the measured one (**Fig. 6(a1) & Fig. 6(a2)**).Subsequently, the volume of the eroded sediment as well as the flushing efficiency would be higher in the experimental model of T8.

4. CONCLUSION

In the present study, a fully three-dimensional numerical model was utilized for reproducing the surface velocity distribution pattern and flushing channel formation in shallow reservoirs. Main outcomes of the study were as follows:

(a) Many hydrodynamic aspects such as jet trajectory, recirculation zones, eddies and the flow distribution pattern, in different shallow reservoir geometries were presented quantitatively by the numerical model. Application of the hydrodynamic module of the numerical model would be beneficial for flood risk management in reservoir areas.

(b) As for the flushing channel formation, a complex dynamic interaction exists between various effective parameters. However, three-dimensional numerical model could successfully reproduce the main governing procedures in flushing channel formation and evolution. In terms of the flushing channel location and Flushing Efficiency (FE), the influence of reservoir width is higher than reservoir length. Thus, higher Shape Factor (SF) leads to higher efficiency of flushing with drawdown. In the case of numerical simulation of flushing with drawdown, the efficiency can be further increased if the non-symmetric inflow pattern, as a kind of perturbation, can be included in the numerical model to initiate wide meandering channel form.

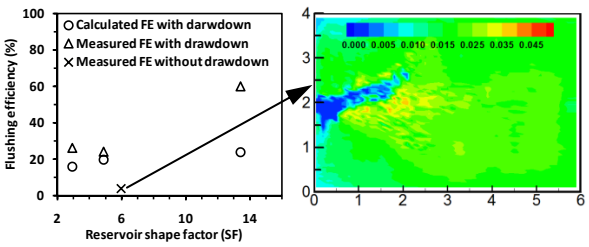

Fig. 8 Left: Measured and calculated FE with drawdown for various reservoir geometries. Right: Illustration of local erosion obtained during the flushing without drawdown.

REFERENCES

1) Morris, G. L., and Fan, J.: Reservoir Sedimentation Handbook: Design and Management of Dams, Reservoirs and Watersheds for Sustainable Use, McGraw-Hill, New York, 1998.
2) White, R.: 2. Review of sedimentation in reservoirs, Thomas Telford, London, 2001.
3) Liu, J., Minami, S., Otsuki, H., Liu, B., and Ashida, K.: Prediction of Concerted Sediment Flushing, *Journal of Hydraulic Engineering*, ASCE, Vol. 130, No. 11, pp. 1089-1096, 2004.
4) Batuca, D. G. and Jordaan, J.M.: Stilling and desilting of reservoirs, A. A. Balkema, Rotterdam, 2000.
5) Kantoush, S. A., Sumi, T., Suzuki, T., and Murasaki, M.: Impacts of sediment flushing on channel evolution and morphological processes: Case study of the Kurobe River, Japan, *Proc.5th* River Flow Conference, Germany, Braunschweig, 2010.
6) Fukuoka, S., Sumi, T., and Horiuchi, S.: Sediment Management on the Arase Dam Removal Project, *Proc.12th* International Symposium on River Sedimentation, Japan, Kyoto, 2013.
7) Shimizu, Y., Itakura, T., and Yamaguchi, H.: Numerical simulation of bed topography of river channels using two-dimensional model, *Proceedings of the Japanese Conference on Hydraulics*, Vol. 31, pp. 689-694, 1987.
8) Uchida, T. and Fukuoka, S.: A computation method for flow over structures, *Advances in River Engineering*, Vol. 18, pp. 351-356, 2012.
9) Fukuoka, S. and Uchida, T.: Toward Integrated Multi-Scale Simulations of Flow and Sediment Transport in Rivers, *Journal of JSCE, Ser. B1 (Hydraulic Engineering),* Vol. 69, No. 4, pp. II_1-II_10, 2013
10) Olsen, N. R. B.: A Three-Dimensional Numerical Model For Simulation of Sediment Movements In Water Intakes With Multi-block Option, Department of Hydraulic and Environmental Engineering, The Norwegian University of Science and Technology, Trondheim, 2012.
11) Launder, B.E. and Spalding D. B.: Lectures in Mathematical Models of Turbulence, Academic Press, London, 1972.
12) Patankar, S.V.: Numerical Heat Transfer and Fluid Flow, McGraw-Hill, New York, 1980.
13) Van Rijn, L. C.: Sediment Transport. Part II: Suspended load Transport, *Journal of Hydraulic Engineering*, ASCE, Vol. 110, No. 11, pp. 1431-1456.
14) Van Rijn, L. C.: Sediment Transport. Part I: Bed load Transport, *Journal of Hydraulic Engineering*, ASCE, Vol. 110, No. 10, pp. 1733-1754.

(Received September 30, 2013)